IMPLEMENTING MULTI-SCALE AGRICULTURAL INDICATORS EXPLOITING SENTINELS

VEGETATION FIELD DATA AND PRODUCTION OF GROUND-BASED MAPS:

MERGUELLIL SITE, TUNISIA
JANUARY – MAY 2014

ISSUE I1.00

EC Proposal Reference N° FP7-311766

Actual submission date : November 2014

Start date of project: 01.11.2012   Duration : 40 months

Name of lead partner for this deliverable: EOLAB

Book Captain: Consuelo Latorre (EOLAB)

Contributing Authors: Fernando Camacho (EOLAB)
Mehrez Zribi, Hassan Ayari, Bernard Mougenot (CESBIO)
Aicha Chahbi (CESBIO-INAT)

Project co-funded by the European Commission within the Seventh Framework Program (2007-2013)		
Dissemination Level		
PU	Public	**X**
PP	Restricted to other programme participants (including the Commission Services)	
RE	Restricted to a group specified by the consortium (including the Commission Services)	
CO	Confidential, only for members of the consortium (including the Commission Services)	

DOCUMENT RELEASE SHEET

Book Captain:	C. Latorre	Date: 03.11.2014	Sign.
Approval:	R. Lacaze	Date: 25.11.2014	Sign.
Endorsement:		Date:	Sign.
Distribution:			

CHANGE RECORD

Issue/Revision	Date	Page(s)	Description of Change	Release
	03.11.2014	All	First Issue	I1.00

TABLE OF CONTENTS

LIST OF FIGURES

LIST OF TABLES

LIST OF ACRONYMS

CCD	Charge coupled devices
CEOS	Committee on Earth Observation Satellite
CEOS LPV	Land Product Validation Subgroup
DG AGRI	Directorate General for Agriculture and Rural Development
DG RELEX	Directorate General for External Relations (European Commission)
DHP	Digital Hemispheric Photographs
ECV	Essential Climate Variables
EUROSTATS	Directorate General of the European Commission
ESU	Elementary Sample Unit
FAPAR	Fraction of Absorbed Photo-synthetically Active Radiation
FAO	Food and Agriculture Organization
FCOVER	Fraction of Vegetation Cover
GCOS	Global Climate Observing System
GEO-GLAM	Global Agricultural Geo- Monitoring Initiative
GIO-GL	GMES Initial Operations - Global Land (GMES)
GCOS	Global Climate Observing System
GMES	Global Monitoring for Environment and Security
GPS	Global Positioning System
IMAGINES	Implementing Multi-scale Agricultural Indicators Exploiting Sentinels
INAT	Institut National Agronomique de Tunisie.
JECAM	Joint Experiment for Crop Assessment and Monitoring
LAI	Leaf Area Index
LDAS	Land Data Assimilation System
LUT	Look-up-table techniques
PROBA-V	Project for On-Board Autonomy satellite, the V standing for vegetation.
RMSE	Root Mean Square Error
SPOT /VGT	Satellite Pour l'Observation de la Terre / VEGETATION
SCI	GMES Services Coordinated Interface
TOA	Top of Atmosphere Reflectance
USGS	U.S. Geological Survey. Science organization.
UNFCCC	United Nations Framework Convention on Climate Change
UTM	Universal Transverse Mercator coordinates system
VALERI	Validation of Land European Remote sensing Instruments
WGCV	Working Group on Calibration and Validation (CEOS)
WGS-84	World Geodetic System

1. BACKGROUND OF THE DOCUMENT

1.1. EXECUTIVE SUMMARY

The Copernicus Land Service has been built in the framework of the FP7 geoland2 project, which has set up pre-operational infrastructures. ImagineS intends to ensure the continuity of the innovation and development activities of geoland2 to support the operations of the global land component of the GMES Initial Operation (GIO) phase. In particular, the use of the future Sentinel data in an operational context will be prepared. Moreover, IMAGINES will favor the emergence of new downstream activities dedicated to the monitoring of crop and fodder production.

The main objectives of ImagineS are to (i) improve the retrieval of basic biophysical variables, mainly LAI, FAPAR and the surface albedo, identified as Terrestrial Essential Climate Variables, by merging the information coming from different sensors (PROBA-V and Landsat-8) in view to prepare the use of Sentinel missions data; (ii) develop qualified software able to process multi-sensor data at the global scale on a fully automatic basis; (iii) complement and contribute to the existing or future agricultural services by providing new data streams relying upon an original method to assess the above-ground biomass, based on the assimilation of satellite products in a Land Data Assimilation System (LDAS) in order to monitor the crop/fodder biomass production together with the carbon and water fluxes; (iv) demonstrate the added value of this contribution for a community of users acting at global, European, national, and regional scales.

Further, ImagineS will serve the growing needs of international (e.g. FAO and NGOs), European (e.g. DG AGRI, EUROSTATS, DG RELEX), and national users (e.g. national services in agro-meteorology, ministries, group of producers, traders) on accurate and reliable information for the implementation of the EU Common Agricultural Policy, of the food security policy, for early warning systems, and trading issues. ImagineS will also contribute to the Global Agricultural Geo-Monitoring Initiative (GEO-GLAM) by its original agriculture service which can monitor crop and fodder production together with the carbon and water fluxes and can provide drought indicators, and through links with JECAM (Joint Experiment for Crop Assessment and Monitoring).

1.2. PORTFOLIO

The ImagineS portfolio contains global and regional biophysical variables derived from multi-sensor satellite data, at different spatial resolutions, together with agricultural indicators, including the above-ground biomass, the carbon and water fluxes, and drought indices resulting from the assimilation of the biophysical variables in the Land Data Assimilation System (LDAS).

The production in Near Real Time of the 333m resolution products, at a frequency of 10 days, using PROBA-V data will be carried out in the Copernicus Global Land Service. It

should start by covering Europe only, and be gradually extended to the whole globe. Meanwhile, ImagineS will perform in parallel off-line production over demonstration sites outside Europe. The demonstration of high resolution (30m) products (Landsat-8 + PROBA-V) will be done over demonstration sites of cropland and grassland in contrasting climatic and environmental conditions.

1.3. SCOPE AND OBJECTIVES

The main objective of this document is to describe the ground database, provided by the CESBIO - Centre d'Etudes Spatiales de la Biosphère, and collected over cereal crops at Merguellil site in Tunisia, and the up-scaling of the ground data carried out by EOLAB to derive high resolution maps of Leaf Area Index (LAI).

LAI is defined as half of the total developed area of leaves per unit ground surface area (m2/m2). We focused on the effective LAI for green elements. One effective LAI (LAIeff) map is produced per campaign, in which the LAIeff is derived from hemispherical digital photography. A binary classification of green elements and soil is proposed, in order to compute the gap fraction at a 57.5° zenith angle.

1.4. CONTENT OF THE DOCUMENT

This document is structured as follows:

- Chapter 2 provides an introduction to the field experiment.
- Chapter 3 provides the location and description of the site.
- Chapter 4 describes the ground measurements, including material and methods, sampling and data processing.
- Chapter 5 describes an evaluation of the sampling.
- Chapter 6 describes the methodology to derive high resolution maps of the biophysical variables, and the results of the high resolution dataset.

1.5. RELATED DOCUMENT

ImagineS_RP7.5_FieldCampaign_   : Field campaign and Data Processing report of the
Mergellil2013   measurements collected in 2013 over Merguellil site.

2. INTRODUCTION

Validation of remote sensing products is mandatory to guaranty that the satellite products meets the user's requirements. Protocols for validation of global LAIeff products are already developed in the context of Land Product Validation (LPV) group of the Committee on Earth Observation Satellite (CEOS) for the validation of satellite-derived land products (Fernandes et al., 2014), and recently applied to Copernicus global land products based on SPOT/VGT observation (Camacho et al., 2013). This generic approach is made of 2 major components:

- The indirect validation: including inter-comparison between products as well as evaluation of their temporal and spatial consistency
- The direct validation: comparing satellite products to ground measurements of the corresponding biophysical variables. In the case of low and medium resolution sensors, the main difficulty relies on scaling local ground measurements to the extent corresponding to pixels size. However, the direct validation is limited by the small number of sites, for that reason a main objective of ImagineS is the collection of ground truth data in demonstration sites.

The content of this document is compliant with existing validation guidelines (for direct validation) as proposed by the CEOS LPV group (Morisette et al., 2006); the VALERI project (http://w3.avignon.inra.fr/valeri/) and ESA campaigns (Baret and Fernandes, 2012). It therefore follows the general strategy based on a bottom up approach: it starts from the scale of the individual measurements that are aggregated over an elementary sampling unit (ESU) corresponding to a support area consistent with that of the high resolution imagery used for the upscaling of ground data. Several ESUs are sampled over the site. Radiometric values over a decametric image are also extracted over the ESUs. This will be later used to develop empirical transfer functions for upscaling the ESU ground measurements (e.g. Martínez et al., 2009). Finally, the high resolution ground based map will be compared with the medium resolution satellite product at the spatial support of the product.

Multi-temporal campaigns (Table 1) to characterize the vegetation biophysical parameters at the Merguellil site were carried out by the CESBIO - Centre d'Etudes Spatiales de la Biosphère and INAT (*Institut National Agronomique de Tunisie*), in the framework of METASIM and RESAMED projects in the SCIMED/MISTRALS French program and AMETHYST project in the TRANSMED-ANR program.

Table 1: Ground Campaigns and Landsat-8 Imagery available.

CAMPAIGN	DATES	IMAGERY
First campaign	21st of January 2014	Landsat-8 TOA (19.01.2014)
Second campaign	14th of February 2014	Cloud contaminated
Third campaign	21st of March 2014	Cloud contaminated
Fourth campaign	15th of April 2014	Landsat-8 TOA (9.04.2014)
Fifth campaign	8th of May 2014	Landsat-8 TOA (11.05.2014)

Ground data file presents 7 multi-temporal campaigns to characterize LAIeff at the Merguellil test site, 5 field campaigns are valid due to the number of ESUs collected (Table 1), while for only two of them HR Biophysical maps have been generated. Both campaigns have free clouds images and its variables have representative values of the ground data: first campaign in January in growing stage of crops and the fourth campaign in April which raises the maximum of phenology trends. Field campaign of May has been discarded for this report due to the low values obtained in the ground dataset; the reason of this fall could be explained with the senescent stage or harvested crops, therefore the information of the fields provided is not enough for evaluating the results.

Team involved in field collection:

Mehrez Zribi, Hassan Ayari, Bernard Mougenot (CESBIO)

Aicha Chahbi (CESBIO-INAT)

Contact: Mehrez Zribi (mehrez.zribi@ird.fr)

3. STUDY AREA

3.1. LOCATION

The experimental Merguellil site is located around the Kairouan plain, situated in central Tunisia (35°33'58.38" N, 9°54'43.78" E). The climate in this region is semi-arid, with an average annual rainfall of approximately 300 mm per year, characterized by a rainy season lasting from October to May, with the two rainiest months being October and March. As is generally the case in semi-arid areas, the rainfall patterns in this area are highly variable in time and space. The mean temperature in Kairouan City is 19.2ºC (minimum of 10.7º in January and maximum of 28.6ºC in August). The mean annual potential evapotranspiration (Penman) is close to 1600 mm.

Figure 1: Location of Merguellil site in Tunisia. Global Map and the study area.

The study area (Figure 1) is defined by a 3x3 km^2 region around the central coordinate (Table 2). Two extended area of 5x5 km^2 and 10x10 km^2 are considered for the Transfer function.

Table 2: Coordinates and altitude of the site.

Site Center	
Geographic Lat/lon, WGS-84 (degrees)	Latitude = 35°33'58.38" N Longitude = 9°54'43.78" E
Altitude	127 m
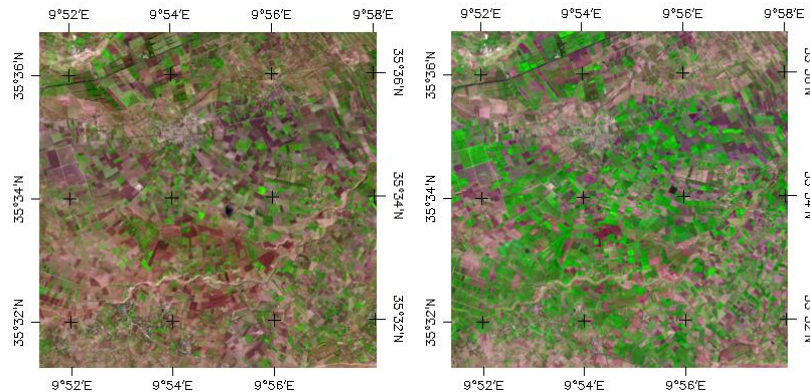
Figure 2: 10x10 km^2 TOA – RGB (SWIR, NIR, RED) false color composition from Landsat images. Left: 21st January 2014. Right: 15th April 2014. Merguellil site in Tunisia.

3.2. DESCRIPTION OF THE SITE.

The landscape is mainly flat and the vegetation in this area is dominated by agriculture (cereals, olive trees, and market gardens). Crops types are wheat, tomatoes, pepper, broad beans, melon, watermelon and olive. Typical field rotation is cereals, forage, broad beans in winter, and vegetables in summer. Land cover changes are observed in some field plots (Figure 3).
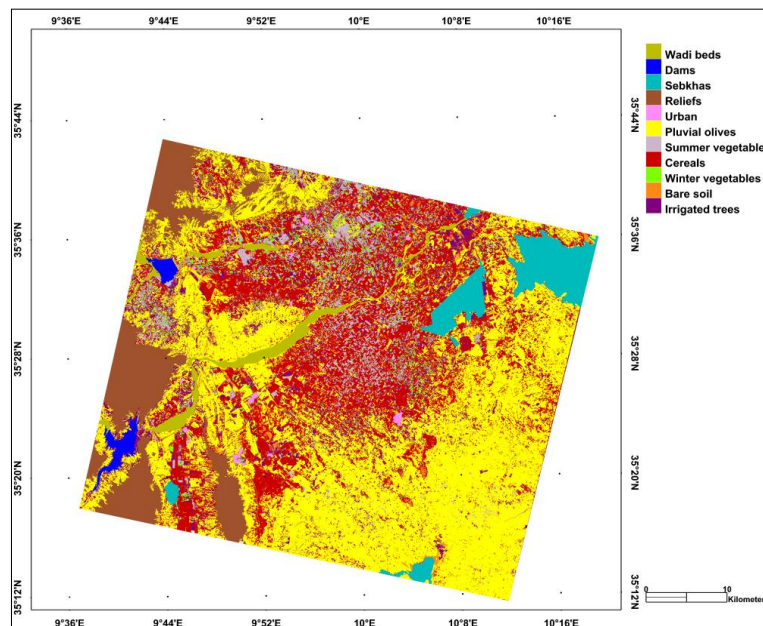
Figure 3: Land use map of the study area. Merguellil site in Tunisia, (2011-2012).

The crop calendar is winter wheat (Dec-June), spring vegetables (March-July) summer vegetables (June-October), trees all year (olive). Their rotation is typical of semi-arid regions. The aquifer of the Kairouan plain represents the largest basin in central Tunisia. It is fed by the infiltration of surface waters during floods in the natural regime, or at the time of dam releases since the construction of the Sidi Saad and El Haouareb dams. Surface and groundwater streams drain into the Sebkha Kelbia, a large salt lake.

4. GROUND MEASUREMENTS

The ground measurements database was acquired and provided by the CESBIO - Centre d'Etudes Spatiales de la Biosphère and INAT-Institut National Agronomique de Tunisie.

4.1. MATERIAL AND METHODS

LAIeff is derived from digital hemispherical photography. The hemispherical photos acquired during the field campaign were processed with the CAN-EYE software developed by INRA (http://www6.paca.inra.fr/can-eye) to derive LAI, FAPAR and FCOVER. It is based on a RGB colour classification of the image to discriminate vegetation elements from background (i.e., gaps). This approach allows exploiting downward-looking photographs for short canopies (background = soil) as well as upward-looking photographs for tall canopies (background = sky). CAN-EYE software processes simultaneously up to of 25 images acquired over the same ESU. Note that the N images were acquired with similar illumination conditions to limit the variation of colour dynamics between images. The processing is achieved in 3 main steps (Weiss et al., 2004). First, image pre-processing is performed, which includes removing undesired objects (e.g. operator, sun glint) and image contrast adjustments to ensure a better visual discrimination between vegetation elements and background. Second, an automatic classification (k-means clustering) is applied to reduce the total number of distinctive colours of the image to 324 which is sufficient to ensure accurate discrimination capacities while keeping a small enough number of colours to be easily manipulated. Finally, a default classification based on predefined colour segmentation is first proposed and then iteratively refined by the user. The allocation of the colours to each class (vegetation elements versus background) is the most critical phase that needs to be interactive because colours depend both on illumination conditions and on canopy elements. At the end of this process a binary image, background versus vegetation elements (including both green and non-green elements) is obtained.

Hemispherical photos allow the calculation of the provided LAIeff measuring gap fraction through an extreme wide-angle camera lens (i.e. 180º) (Weiss et al., 2004). It produces circular images that record the size, shape, and location of gaps, either looking upward from within a canopy or looking downward from above the canopy. A binary classification of green elements and soil is proposed, in order to compute the gap fraction at a 57.5° zenith angle, from which an estimation of the LAIeff is then derived (Demarez et al., 1998).

4.2. SPATIAL SAMPLING SCHEME

A total of 15 ESUs were characterized during the field campaigns. A pseudo-regular sampling was used within each ESU of approximately 20x20 m^2. The centre of the ESU was geo-located using a GPS. The number of hemispherical photos per ESU ranges between 12 and 15.

Figure 4: Distribution of the sampling units over 5x5 km^2 area. Common ESUs considered in all campaigns. Merguellil – Tunisia, 2014.

Table 3 summarizes the number of sampling units (ESUs) per each field campaign acquired during 2014.

Table 3: Summary of the field measurements in Merguellil – Tunisia, 2014.

Field campaings	Number of ESU's
21st of January 2014	15
14th of February 2014	15
21st of March 2014	14
15th of April 2014	15
8th of May 2014	15

4.3. CONTENT OF THE GROUND DATASET

Each ESU is described according to an agreed format. For this purpose a template file has been used (Table 4).

Table 4: The File template used to describe ESUs with the ground measurements.

Column	Var.Name		Comment
1	Plot #		Number of the field plot in the site
2	Plot Label		Label of the plot in the site
3	ESU #		Number of the Elementary Sampling Unit (ESU)
4	ESU Label		Label of the ESU in the campaign
5	Northing Coord.		Geographical coordinate: Latitude (⁰), WGS-84
6	Easting Coord.		Geographical coordinate: Longitude (⁰), WGS-84
7	Extent (m) of ESU (diameter)		Size of the ESU [1]
8	Land Cover		Detailed land cover
9	Start Date (dd/mm/yyyy)		Starting date of measurements
10	End Date (dd/mm/yyyy)		Ending date of measurements
11	LAIeff	Method	Instrument
12		Nb. Replications	Number of Replications
13		PRODUCT	Methodology
14		Uncertainty	Standard deviation

Five field campaigns have been performed from January to May, 2014. Due to the quality of imagery collection, only two of them have been considered for up-scaling and validation.

Figure 5, 6 and 7, show the measurements obtained during the field experiment. Figure 5 shows the distribution of measurements for all field campaigns by ESUs. Distribution of LAIeff values varies from 0 to 1 for January Field campaign, and from 0 to 7 for the campaigns of March and April, 2014.
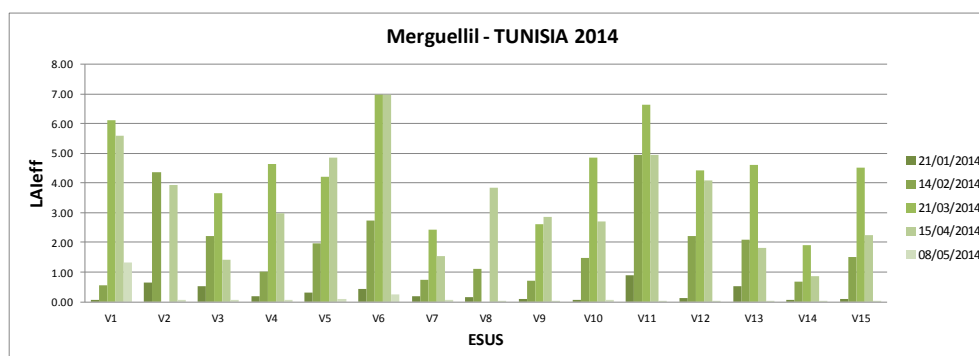
Figure 5: LAIeff measurements acquired in Merguellil site during all campaigns of 2014.

Considered fields are a majority of wheat crops. Figures 6 and 7 show the distribution of the field campaigns of January (Figure 6) and April (Figure 7). First campaign has LAIeff values lower than 1, that corresponds to the beginning part of the growing season.
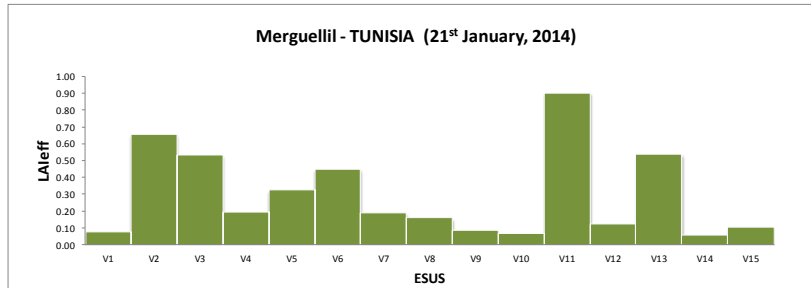
Figure 6: LAIeff measurements acquired in Merguellil site on 21st January, 2014.
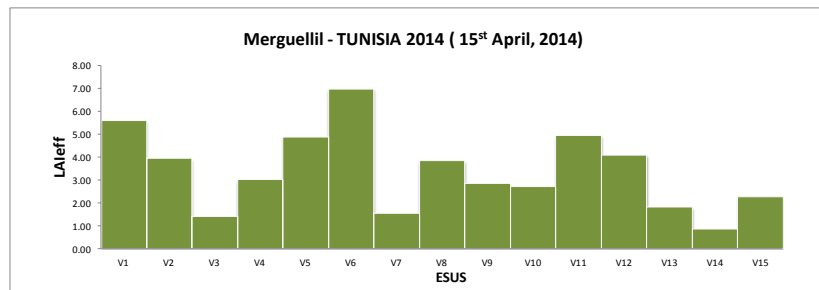
Figure 7: LAIeff measurements acquired in Merguellil site on 15th April, 2014.
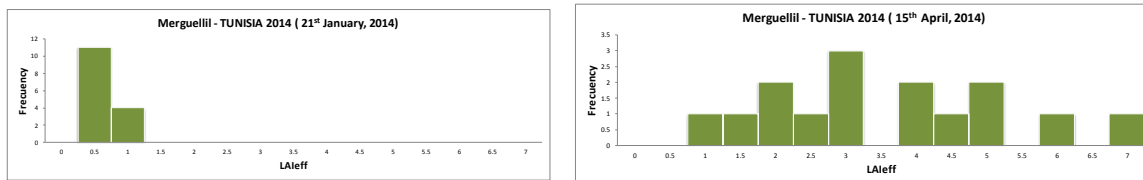
Figure 8: Distribution of the measured biophysical variables over the ESUs. Left: First Campaign (21st January, 2014). Right: Fourth Campaign (15th April, 2014), Merguellil, Tunisia.

Figure 9 shows the distribution values of LAIeff and NDVI-TOA by ESUs in the two selected field campaigns. Good correspondence between NDVI-TOA and LAIeff are obtained.

21ˢᵗ January 2014   **15ᵗʰ April 2014**
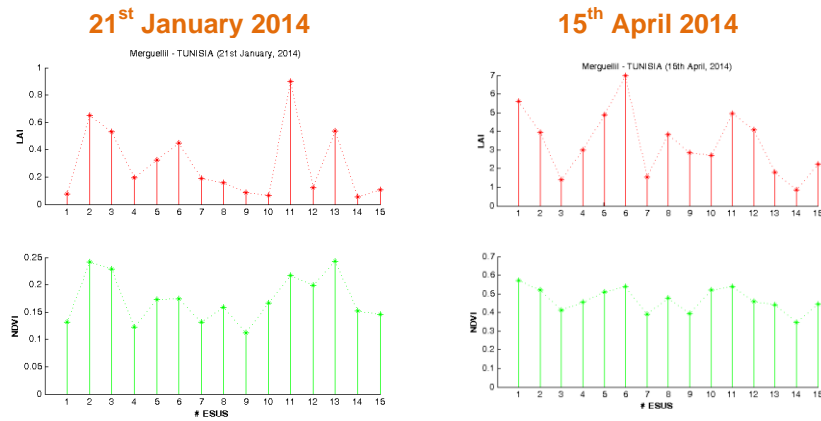
Figure 9: LAIeff and NDVI – TOA measurements acquired in Merguellil site during the selected campaigns of 2014, distributed by ESUs.

5. EVALUATION OF THE SAMPLING

5.1. PRINCIPLES

Based on previous field activities (see ImagineS_FieldCampaign_Merguellil2013 report), the data set sampling was concentrated in the most representative crops, wheat and barley. The number of ESUs was of 15 for the first and fourth campaigns.

5.2. EVALUATION BASED ON NDVI VALUES

The sampling strategy is evaluated using the Landsat-8 image by comparing the NDVI distribution over the site with the NDVI distribution over the ESUs (Figure 10). As the number of pixels is drastically different for the ESU and whole site (WS) it is not statistically consistent to directly compare the two NDVI histograms. Therefore, the proposed technique consists in comparing the NDVI cumulative frequency of the two distributions by a Monte-Carlo procedure which aims at comparing the actual frequency to randomly shifted sampling patterns. It consists in:

   1. computing the cumulative frequency of the N pixel NDVI that correspond to the exact ESU locations; then, applying a unique random translation to the sampling design (modulo the size of the image)

   2. computing the cumulative frequency of NDVI on the randomly shifted sampling design

   3. repeating steps 2 and 3, 199 times with 199 different random translation vectors.

This provides a total population of N = 199 + 1(actual) cumulative frequency on which a statistical test at acceptance probability 1 - α = 95% is applied: for a given NDVI level, if the actual ESU density function is between two limits defined by the $N\alpha\,/\,2$ = 5 highest and lowest values of the 200 cumulative frequencies, the hypothesis assuming that WS and ESU NDVI distributions are equivalent is accepted, otherwise it is rejected.

Figure 10 shows the NDVI distribution. For the first campaign, the distribution of the measured low values is close to highest estimation while the distribution of the measured high NDVI values is more proximate to lower estimation. Fourth campaign has the opposite response. Both are good over the whole site.

21st January 2014 **15th April 2014**
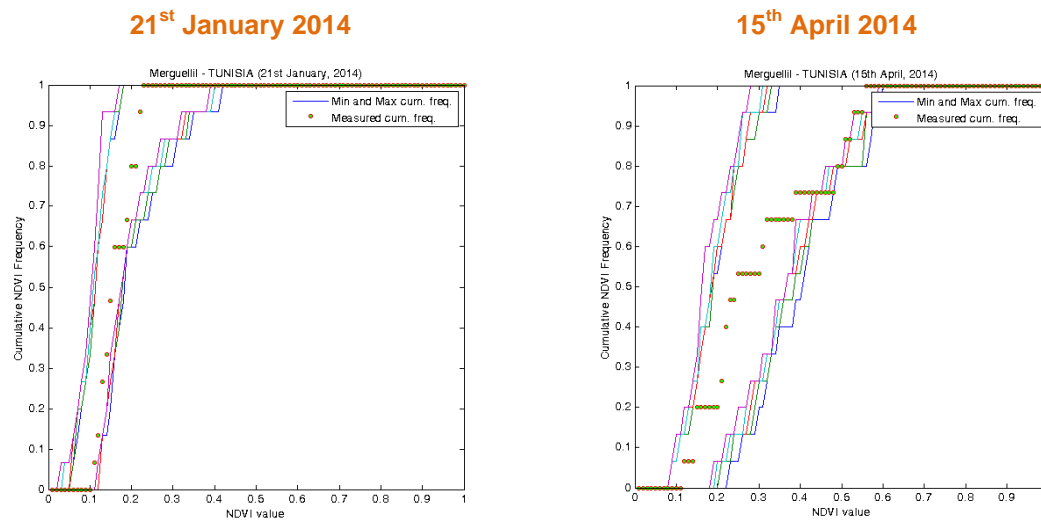
Figure 10: Comparison of NDVI distribution between ESUs and over the whole image. Left: First Campaign (21st January, 2014). Right: Fourth Campaign (15th April, 2014).

5.3. EVALUATION BASED ON CONVEX HULL: PRODUCT QUALITY FLAG.

The interpolation capabilities of the empirical transfer function used for upscaling the ground data using decametric images is dependent of the sampling (Martinez et al., 2009). A test based on the convex hulls was also carried out to characterize the representativeness of ESUs and the reliability of the empirical transfer function using the different combination of the selected bands (green, red, NIR and SWIR) of the Landsat-8 image. A flag images is computed over the reflectances. The result on convex-hulls can be interpreted as:

● pixels inside the 'strict convex-hull': a convex-hull is computed using all the Landsat-8 reflectances corresponding to the ESUs belonging to the class. These pixels are well represented by the ground sampling and therefore, when applying a transfer function the degree of confidence in the results will be quite high, since the transfer function will be used as an interpolator;

● pixels inside the 'large convex-hull': a convex-hull is computed using all the reflectance combinations (± 5% in relative value) corresponding to the ESUs. For these pixels, the degree of confidence in the obtained results will be quite good, since the transfer function is used as an extrapolator (but not far from interpolator);

● pixels outside the two convex-hulls: this means that for these pixels, the transfer function will behave as an extrapolator which makes the results less reliable. However, having a priori information on the site may help to evaluate the extrapolation capacities of the transfer function.

Figure 11 shows the results of the Convex-Hull test (i.e., Quality Flag image) for the Merguellil site over a 10x10 km^2 and 5x5 km^2 areas around the central coordinate site. The flag maps show there is a big extrapolation of the transfer function all over the site. The strict and large convex-hulls are better for the first campaign (34% and 31%), while for fourth one are 17% and 24% respectively. Therefore, because the soil is not accounted in the ground data, a mask has been created to filter soil areas with a NDVI-TOA lower than 0.124 for first campaign and lower than 0.18 for the fourth one.

Table 5: Percentages over the two areas over the test site of Merguellil – Tunisia. (0: extrapolation of TF, 1: strict convex hull, 2: large convex hull, 3: soil mask).

Field Campaigns, 2014	Quality Flags (%)							
DATES	10x10 km^2				5x5 km^2			
Convex hull values	0	1	2	3	0	1	2	3
21st January	32%	27%	7%	34%	32%	25%	6%	37%
15th April	62%	14%	3%	21%	59%	21%	3%	17%

21st January 2014   15th April 2014

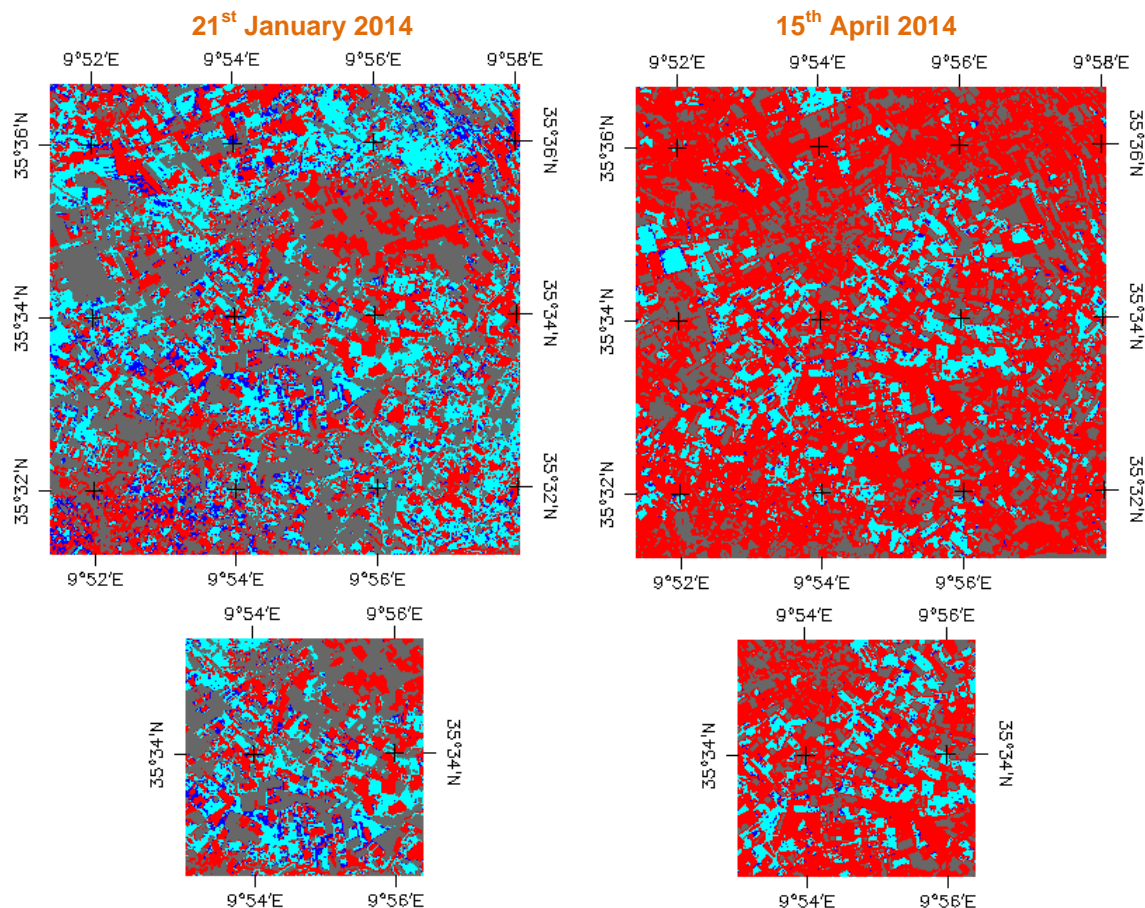**Figure 11: Convex Hull test over 10x10 km^2 (Top) and 5x5km^2 (Bottom) area centered at the site: clear and dark blue correspond to the pixels belonging to the 'strict' and 'large' convex hulls. Red corresponds to the pixels for which the transfer function is extrapolating and grey to the soil mask. Left: First Campaign (21st January, 2014); Right: Fourth Campaign (15th April, 2014), Merguellil, Tunisia.**

6. ESTIMATION OF THE HIGH RESOLUTION MAPS

6.1. IMAGERY

Cloud free Landsat-8 images were acquired the 19th January and 9th April 2014 (see Table 6 for acquisition properties). Four spectral bands were selected from 500 nm to 1750 nm with a nadir ground sampling distance of 30 m. Therefore, for the transfer function analysis, the input satellite data used is Top of Atmosphere (TOA) reflectance. The original projection is UTM 32 North, WGS-84.

Table 6: Acquisition properties of Landsat-8 data used for retrieving high resolution maps.

Landsat-8 METADATA		
Platform / Instrument	Landsat- 8 / OLI_TIRS	
Path	191	
Row	35	
Spectral Range	B3(green) : 0.53-0.59 µm B4(red) : 0.64-0.67 µm B5(NIR) : 0.85-0.88 µm B6(SWIR1) : 1.58-1.65 µm	
	January 2014 campaign	April 2014 campaign
Acquisition date	2014-01-19 09:56:07	2014-04-09 09:55:04
Illumination Azimuth angle	154.721º	140.263º
Illumination Elevation angle	29.653º	55.690º
Ground Control Points Verify	121	130
Geometric RMSE Verify (m)	3.880	4.327

6.2. THE TRANSFER FUNCTION

6.2.1. The regression method

If the number of ESUs is sufficient, multiple robust regression 'REG' between ESUs reflectance (or Simple Ratio) and the considered biophysical variable can be applied (Martínez et al., 2009): we used the 'robustfit' function from the Matlab statistics toolbox. It uses an iteratively re-weighted least squares algorithm, with the weights at each iteration computed by applying the bisquare function to the residuals from the previous iteration. This algorithm provides lower weight to ESUs that do not fit well.

The results are less sensitive to outliers in the data as compared with ordinary least squares regression. At the end of the processing, two errors are computed: weighted RMSE

(RW) (using the weights attributed to each ESU) and cross-validation RMSE (RC) (leave-one-out method).

As the method has limited extrapolation capacities, a flag image (Figure 11), based on the convex hulls, is included in the final ground based map in order to inform the users on the reliability of the estimates.

6.2.2. Band combination

Figure 12 shows the results obtained for all the possible band combinations using the reflectance. Attending specifications of lower RMSE, it has been chosen for both campaigns: band 1 (green), band 2 (red) band 3 (Near Infrared) and band 4 (Short Wave Infrared) combination of (1,2,3,4) = (G, R, N, S).

This combination on reflectance was selected since provide a good compromise between the cross-validation RMSE, the weighted RMSE (lowest value) and the number of rejected points as well.

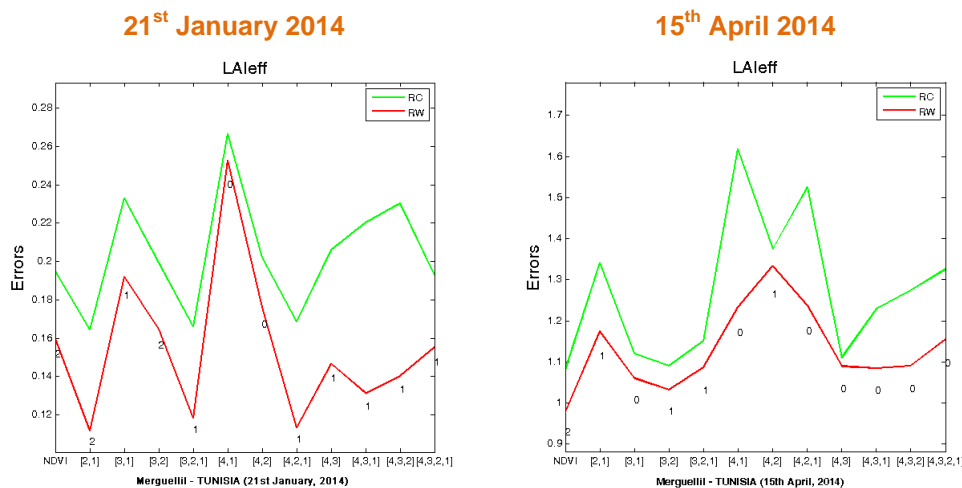**21st January 2014**   **15th April 2014**

Figure 12: Test of multiple regression applied on different band combinations. Band combinations are given in abscissa (1=G, 2=RED, 3=NIR and 4=SWIR). The weighted root mean square error (RMSE) is presented in red along with the cross-validation RMSE in green. The numbers indicate the number of data used for the robust regression with a weight lower than 0.7 that could be considered as outliers. Left: First Campaign (21st January, 2014); Right: Fourth Campaign (15th April, 2014), Merguellil, Tunisia.

6.2.3. The selected Transfer Function

The applied transfer function for LAIeff is detailed in Table 7, along with its weighted and cross validated errors.

Table 7: Transfer function applied to the whole site for LAIeff for weighted RMSE (RW), and for cross-validation RMSE (RC).

Variable	Band Combination	RW	RC
21st January			
LAIeff	$- 0.96033 + 0.00022 \cdot (SWIR) - 0.00125 \cdot (NIR)$ $- 0.00134 \cdot (R) + 0.00139 \cdot (G)$	0.143	0.155
15th April, 2014			
LAIeff	$4.35548 - 0.00029 \cdot (SWIR) + 0.00042 \cdot (NIR)$ $- 0.00015 \cdot (R) - 0.00062 \cdot (G)$	1.073	1.155

Figure 13 shows scatter-plots between ground observations and their corresponding transfer function (TF) estimates for the selected bands combination. A good correlation is observed for the LAIeff with points distributed along the 1:1 line, and no systematic errors.

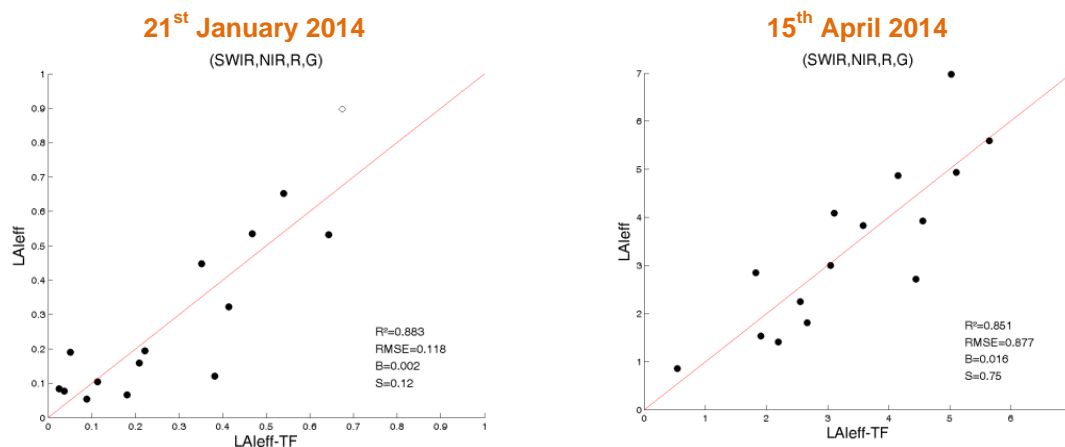**Figure 13: LAIeff results for regression on reflectance using 4 bands combination. Full dots: Weight>0.7. Empty dots: 0<Weight<0.7. Left: First Campaign (21st January, 2014); Right: Fourth Campaign (15th April, 2014), Merguellil, Tunisia.**

6.3.   THE HIGH RESOLUTION GROUND BASED MAPS

The high resolution maps are obtained applying the selected transfer function of each campaign (Table 5) to the Landsat-8 TOA reflectance. Figure 14 and 15 present the TF biophysical variables over 10x10 km^2 and 5x5 km^2 areas. Figure 11 shows the Quality Flag included in the final product.
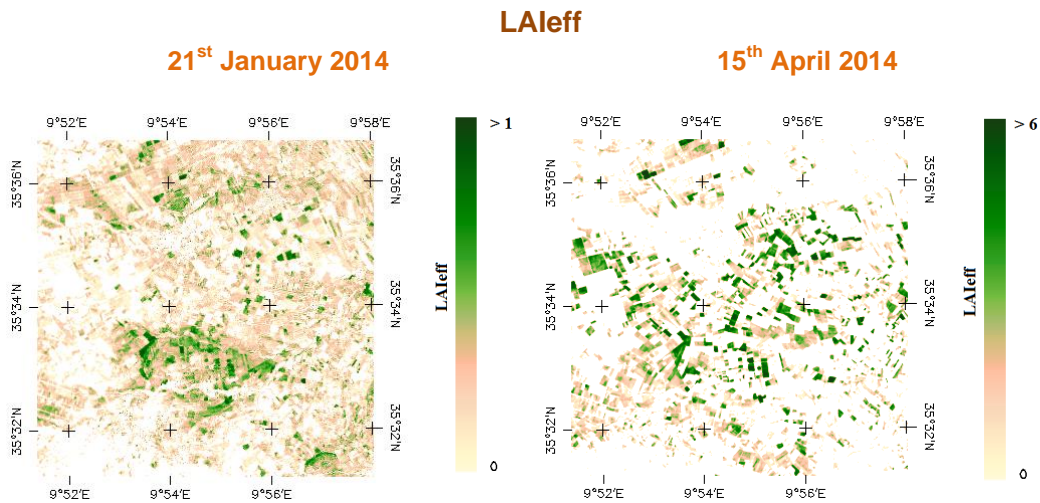

Figure 14: HR LAIeff maps (10x10 km^2) applied on the Merguellil site. Left: First Campaign (21st January, 2014); Right: Fourth Campaign (15th April, 2014), Merguellil, Tunisia.

Figure 15: HR LAIeff maps (5x5 km^2) applied on the Merguellil site. Left: First Campaign (21st January, 2014); Right: Fourth Campaign (15th April, 2014), Merguellil, Tunisia.
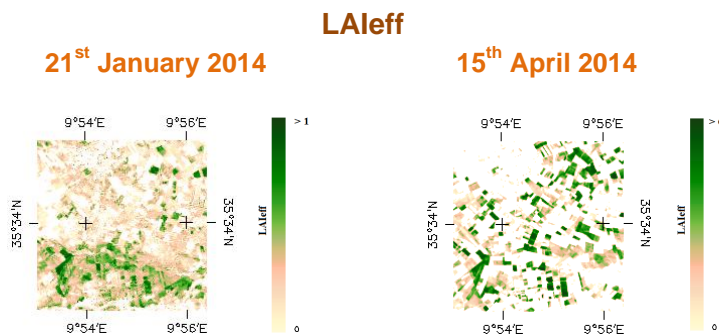
Figure 15 summarizes these ground-based high resolution maps over the 5x5 km^2 study area. These maps are provided for validation of satellite products at different resolutions (see table 8)

6.3.1.   Mean Values

Mean values of a 3x3 km^2 area centred in the test site are provided for validation of 1 km satellite products in agreement with the CEOS OLIVE direct dataset (Table 8). For the

validation of coarser resolutions product (e.g. MSG products) a larger area should be considered. For this reason, maps are also provided at 5x5 km^2, and 10x10 km^2.

Table 8: Mean values and standard deviation (STD) of the HR biophysical maps for the 3x3km^2 Merguellil site.

Field Campaigns, 2014	3x3 km^2	
DATES	Mean	STD
21st January	0.181	0.169
15th April	0.928	1.462

Table 9 describes the content of the geo-biophysical maps in the nomenclature: "BIO_YYYYMMDD_SENSOR_Site_ETF_Area" files, where:

BIO stands for Biophysical (LAIeff)

SENSOR = LANDSAT8

YYYYMMDD = Campaign date

Site = Merguellil

ETF stands for Empirical Transfer Function

Area = window size 10x10 km^2 and 5x5 km^2

Table 9: Content of the dataset.

Parameter	Dataset name	Range	Variable Type	Scale Facor	No Value
LAIeff	LAIeff	[0, 7]	Integer	1000	-1
Quality Flag	QFlag	0,1,2,3 (*)	Integer	N/A	-1

[*] 0 means extrapolated value (low confidence), 1 strict interpolator (best confidence), 2 large interpolator, 3 soil values

7. CONCLUSIONS

The FP7 ImagineS project continues the innovation and development activities to support the operations of the Copernicus Global Land service. One of the ImagineS demonstration sites is located in Merguellil (Tunisia). High resolution maps of main biophysical variables of the vegetation canopy have been derived over this agriculture area, according with the CEOS LPV methodology for validation of low resolution satellite sensors.

This study show the ground data collected during five field campaigns performed from January to May of 2014. Two of them (21st January and 15th April, 2014) have been considered for up-scaling due to the quality of available imagery. The dataset includes 15 elementary sampling units where digital hemispherical photographs were taken and processed with the CAN-EYE software to provide effective LAI values to characterize the crops of the area (wheat and barley).

High resolution ground based maps of the biophysical variable LAIeff have been produced over the 5x5 km^2 validation area and the extended 10x10 km^2 area. Ground-based maps have been derived using high resolution imagery (Landsat-8). Transfer functions have been calculated by multiple robust regressions between ESUs reflectance and the biophysical variable. The spectral bands combination to minimize RMSE was band 1 (green), band 2 (red) band 3 (Near Infrared) and band 4 (Short Wave Infrared) combination. The RMSE values are 0.118 and 0.877 for the first and fourth campaign respectively.

Additionally, a quality flag map based on the convex hull test is provided, showing 31 % (first campaign) and 24% (fourth campaign) of the Merguellil site (5x5 km^2 area) belongs to the transfer function considered as an interpolator. A mask has been created to filter soil areas with a NDVI lower than 0.124 (January) and 0.18 (April). The percentage of soil pixels identified with this rule is 37% for the first campaign (January) and 17% for the fourth campaign (April).

The biophysical variable maps are available in geographic (UTM 32 North projection WGS-84) coordinates at 30m resolution over the 10x10 km^2 and 5x5 km^2. The means and standard deviation for LAIeff were calculated over the 3x3 km^2 area. The mean values obtained for first and fourth campaigns are 0.181 and 0.928, respectively.

8. ACKNOWLEDGEMENTS

9. REFERENCES

Baret, F. and Fernandes, R. (2012). Validation Concept. VALSE2-PR-014-INRA, 42 pp.

Camacho, F., Cernicharo, J., Lacaze, R., Baret, F., and Weiss, M. (2013). GEOV1: LAI, FAPAR Essential Climate Variables and FCOVER global time series capitalizing over existing products. Part 2: Validation and intercomparison with reference products. *Remote Sensing of Environment, 137: 310-329.*

Demarez, V., Duthoit, S., Baret, F., Weiss, M. and Dedieu, G. (2008). Estimation of leaf area and clumping indexes of crops with hemispherical photographs. *Agricultural and Forest Meteorology. I48, 644-655.*

Fernandes, R., Plummer, S., Nightingale, J., et al. (2014). Global Leaf Area Index Product Validation Good Practices. CEOS Working Group on Calibration and Validation - Land Product Validation Sub-Group. *Version 2.0: Public version made available on LPV website.*

Martínez, B., García-Haro, F. J., & Camacho, F. (2009). Derivation of high-resolution leaf area index maps in support of validation activities: Application to the cropland Barrax site. *Agricultural and Forest Meteorology, 149, 130–145.*

Miller, J.B. (1967). A formula for average foliage density. Aust. J. Bot., 15:141-144

Morisette, J. T., Baret, F., Privette, J. L., Myneni, R. B., Nickeson, J. E., Garrigues, S., et al. (2006). Validation of global moderate-resolution LAI products: A framework proposed within the CEOS land product validation subgroup. IEEE Transactions on Geoscience and Remote Sensing, 44, 1804–1817.

Latorre, C., Sanchez, J.,Camacho, F., Zribi, M., Ayari, H., Mougenot,B., Chahbi, A. "Vegetation Field Data and Production of Ground-Based Maps: Merguellil site, Tunisia. 8th March and 3rd May, 2013" report.

Weiss, M., Baret, F., Smith, G.J., Jonckheere, I. and Coppin, P., (2004). Review of methods for in situ leaf area index (LAI) determination. Part II. Estimation of LAI, errors and sampling. *Agricultural and Forest Meteorology. 121, 37–53.*

Weiss M. and Baret F. (2010). CAN-EYE V6.1 User Manual

Welles, J.M. and Norman, J.M., 1991. Instrument for indirect measurement of canopy architecture. Agronomy J., 83(5): 818-825.